INSTITUTE OF PHYSICS PUBLISHING MEASUREMENT SCIENCE AND TECHNOLOGY

Meas. Sci. Technol. **16** (2005) 46–53 doi:10.1088/0957-0233/16/1/007

PVD synthesis and high-throughput property characterization of Ni–Fe–Cr alloy libraries

A Rar[1,2], J J Frafjord[1,2], Jason D Fowlkes[2], E D Specht[1], P D Rack[2], M L Santella[1], H Bei[1,2], E P George[1,2] and G M Pharr[1,2]

[1] Metals and Ceramics Division, Oak Ridge National Laboratory, Oak Ridge, TN 37831, USA
[2] Department of Materials Science and Engineering, The University of Tennessee, Knoxville, TN 37996, USA

Received 15 April 2004, in final form 21 September 2004
Published 16 December 2004
Online at stacks.iop.org/MST/16/46

Abstract
Three methods of alloy library synthesis, thick-layer deposition followed by interdiffusion, composition-spread codeposition and electron-beam melting of thick deposited layers, have been applied to Ni–Fe–Cr ternary and Ni–Cr binary alloys. Structural XRD mapping and mechanical characterization by means of nanoindentation have been used to characterize the properties of the libraries. The library synthesis methods are compared from the point of view of the structural and mechanical information they can provide.

Keywords: combinatorial, alloy library, Ni, Fe, Cr, nanoindentation, XRD, PVD, high throughput, x-ray diffraction, pulsed vapour deposition

(Some figures in this article are in colour only in the electronic version)

1. Introduction

The development of methods for high-throughput analysis of binary and ternary alloy systems is a subject of great interest in different areas of material science since combinatorial methods were discovered in the 1970s [1–5]. Effective application of combinatorial alloy library design first requires methods for quick synthesis of alloy libraries covering a wide (or even full) range of possible alloy compositions. Second, the library must reproduce the relevant properties of the bulk materials and allow for quick and effective measurements of important properties. The properties of interest in this investigation are phase composition and mechanical properties, including the mechanical properties of non-equilibrium phases and thin films that may be different from the equilibrium and bulk material properties. These latter properties may be important for MEMS device fabrication [6].

We investigate the applicability of three methods to Ni–Fe–Cr ternary and Ni–Cr binary library synthesis: deposition of thick Cr, Fe and Ni layers followed by interdiffusion [7], composition-spread codeposition [8] and a new method based on electron-beam melting of a thick Cr or Ni layer deposited on a Ni or Cr substrate, respectively. Ni–Fe–Cr was selected as a model alloy system because it is the basis of a wide variety of commercially important alloys such as stainless steels. As such, this alloy system has been extensively studied, and its structure and properties are well known [9].

2. Methods of alloy library synthesis

The synthesis of libraries by means of thick film deposition and interdiffusion was described in detail in [7] and is shown schematically in figure 1. Specimens of Ni–Fe–Cr were prepared by depositing films onto 50 mm diameter sapphire substrates followed by annealing in vacuum to interdiffuse the layers. Metal deposition was performed in an electron-beam evaporation system equipped with a sliding shutter and a sample rotation stage. A typical background pressure was about 10^{-6} Torr, and the deposition rate measured with a quartz microbalance was approximately 3 nm s^{-1} for Cr and 0.3 nm s^{-1} for Fe and Ni. Layers of Cr, Fe and Ni were sequentially deposited using the sliding shutter to create a

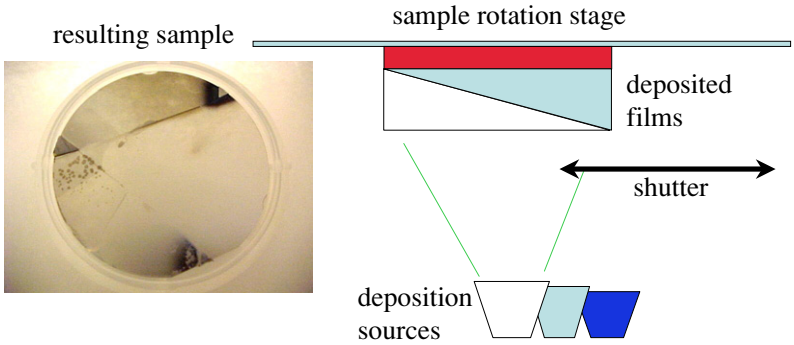

Figure 1. Schematic showing sample ternary alloy library preparation with thick film deposition and interdiffusion. A photo of the resulting sample is shown at the left.

Figure 2. Sample preparation by codeposition from three sputtering sources.

thickness gradient in each layer. The shutter was moved at a constant rate such that the thickness of each layer increased linearly with position to a maximum of about 1.7 μm at the thick end. After finishing a layer, the sample was rotated by 120° about the substrate centre, and a layer of a different alloying component was deposited. The total thickness of the deposited layers was limited by the maximum thickness measurable by the quartz microbalance (about 5 μm). After deposition, the layers were interdiffused by annealing. The resulting sample is shown on the left side of figure 1. This sample consisted of a triangular region with a constant thickness of about 1.7 μm and compositions spanning the entire ternary phase diagram and binary regions with non-constant thickness around the samples. Similar methods of library fabrication based on multilayer deposition have been used by others [10].

Composition-spread codeposition is probably the most popular method of library synthesis. The experimental setup used here corresponds to that used in an earlier publication [11]. The alloy films were deposited using an RF magnetron sputtering system onto 100 mm diameter sapphire substrates. Figure 2 shows the three-source assembly illustrating the source positions relative to the substrate. The sputtering system has three 50 mm sources that were simultaneously sputtered onto the fixed substrate. The iron and nickel sources were oriented 180° apart in the chamber, and the chromium target was oriented 90° from both the iron and nickel targets. All the target centres were 16.5 cm from the substrate centre and were tilted at 32° relative to the substrate normal to create a composition gradient across the substrate.

For each deposition, the base pressure was nominally 7×10^{-7} Torr and the processing pressure was 10^{-3} Torr of argon. The sputtering powers for the Fe, Cr and Ni targets were 160 W, 60 W and 60 W, respectively, and each film was deposited for 3 h. Film thicknesses were about 2 μm for each film. No deliberate heating was applied to the substrate during the deposition of the films; however the plasma produced nominal heating of the substrate (about 100 °C). A total of five samples were sputter deposited, and all except one were vacuum annealed for 2 h at temperatures of 200, 400, 600 and 800 °C.

Library synthesis by means of electron-beam melting was performed using a new technique. Nickel or chromium substrates with a purity of 99.999% were polished with 6, 3 and 1 μm diamond suspensions and cleaned in acetone and ethanol. A Cr or Ni layer, with or without thickness gradients, was deposited onto the nickel or chromium substrate, respectively, by PVD. The deposition rate was about 1.2–1.6 nm s^{-1}, and the total thickness of the deposited film varied from 0 to 10 μm. Electron-beam welding (EBW) was performed to alloy the film with the substrate in a Leybold–Heraeus electron-beam welder in vacuum ($<3.2 \times 10^{-4}$ Torr). For all the libraries, the composition of the resulting alloy was analysed with energy dispersive x-ray spectrometry (EDS). The libraries cover the alloy composition from Ni to Cr. The region with high Cr concentration was prepared by Ni deposition on Cr and vice versa. The reference bulk samples were also prepared by arc melting and casting.

An optical image of a typical cross section of a welded sample is shown in figure 3. The alloyed area is easily distinguished from the Ni matrix by the grain structure of the region that was melted. The Cr composition on the cross section within the alloyed region was found to be uniform by means of EDS.

3. High-throughput library analysis

Among the parameters of interest for materials scientists are structure and mechanical properties. The high-throughput

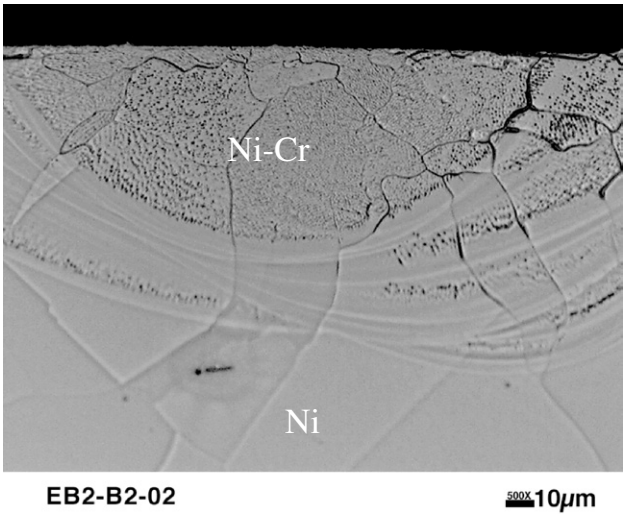

Figure 3. Optical cross section of typical sample made by electron-beam welding.

analysis of these properties of the alloy libraries is probably a bigger challenge than the alloy library preparation. A number of limitations on the methods of sample characterization originate from the combinatorial nature of the sample and the thin film or line form of the samples. The combinatorial nature of the sample requires analysis of a few thousand points to produce a map of the properties and quick analysis of the properties at each point is essential. This made traditional x-ray diffraction measurements impractical because the typical time for data acquisition at each point is more than a minute. The method of choice for mapping of the structure was synchrotron-based x-ray diffraction.

The measurements of mechanical properties are also strongly limited by the small sample size. We know of only a few methods that can be used to measure mechanical properties for such samples. Elastic modulus and hardness may be measured by nanoindentation [12] and elastic modulus by atomic force acoustic microscopy [13] and ultrasonic microscopy [14]. Nanoindentation was selected because it is a more conventional method, has a higher acquisition rate and gave hardness measurements.

The x-ray diffraction measurements were described in detail in [15]. The experimental setup is outlined in figure 4. Diffraction and fluorescence data were collected using the bending magnet beamline X33-BM at the Advanced Photon Source (APS). The focused beam size with energy 12 keV was 1.0 mm × 0.25 mm in size, providing a 1.0 mm × 1.0 mm footprint on the sample when incident at a 15° glancing angle. The sample was mapped by rastering in 1 and 2 mm steps for the 50 and 100 mm diameter samples, respectively. The composition range of elements within one spot was about 2 at% for diffused samples and about 1 at% for codeposited samples. Data were collected for 1–2 s at each point.

Fluorescence spectra were acquired using a Si drift detector with a resolution of 165 eV at 6.4 keV. The detector viewed the sample at a 15° glancing angle, the angle of the incident x-rays. The integrated counts in the Cr, Fe and Ni K lines were measured by least-squares fitting to Gaussian line shapes and recalculated to obtain composition. The corners of the ternary diagram were used as internal standards.

Diffraction patterns were taken using a 1024 × 1024 pixel CCD detector. A typical diffraction pattern formed on the CCD is shown in the inset in figure 4. The CCD image was converted to a standard diffraction pattern which is shown in the right panel together with the measured composition. This set of data was used for identification of the phase location on the ternary phase diagram.

Nanoindentation experiments were performed using a commercial nanoindentation system with a Berkovich indenter in the continuous stiffness mode [12].

4. Experimental results for composition and phase distribution

The interdiffused samples easily covered all possible ternary and binary compositional spreads with an almost linear composition dependence on position [15]. The resulting phase distribution for a sample interdiffused by annealing at 875 °C is shown in figure 5 along with a calculated ternary phase diagram at the same temperature. The diagram was calculated using the PANDAT^{TM} Software Package [16] and SSOL2-SGTE Solutions Database [17]. The phase diagram measured from the experimental library is in reasonable agreement with the theoretical prediction. The possible sources of discrepancy are changes during the sample cooling and accuracy of the measurements, as have been discussed elsewhere [7, 15, 18].

For the codeposited samples the composition spread is smaller, and the phase distribution is complicated by a non-equilibrium phase observed after annealing at low temperatures. The measured locations of phases in the codeposited samples are shown in figure 6: (*a*) before annealing, and for 2 h post-deposition annealing temperatures of (*b*) 200 °C, (*c*) 400 °C, (*d*) 600 °C and (*e*) 800 °C. The area of the non-equilibrium phase is indicated by grey shading. This phase was identified as having the α-Mn structure [19], but it must be mentioned that another structure for this metastable phase is the γ-brass structure with a bcc cell containing 52 atoms [20]. The diffraction pattern of γ-brass structure is similar to α-Mn. We have not yet acquired enough data to determine which structure was observed. Other phase boundaries are indicated by the heavy lines. The light lines indicate the edge of the wafer.

Figure 6(*f*) shows for comparison the measured phase diagram for a smaller 50 mm wafer without annealing as was reported in [11]. Increasing the sample size from 50 to 100 mm, which is the maximum possible size for this PVD apparatus, significantly increases the observed composition range of the ternary diagram. However, only about 30% of the possible compositions may be prepared on one substrate. This will not be a significant disadvantage for the practical usage of this method, if investigations are devoted to improvements of the properties of known alloy systems for which only small composition variations are required. Such an application will additionally benefit from good reproducibility of the sample preparation provided by this method. The composition spanned by the film varies by only a few atomic per cent from run to run, indicating consistency of both deposition and analysis.

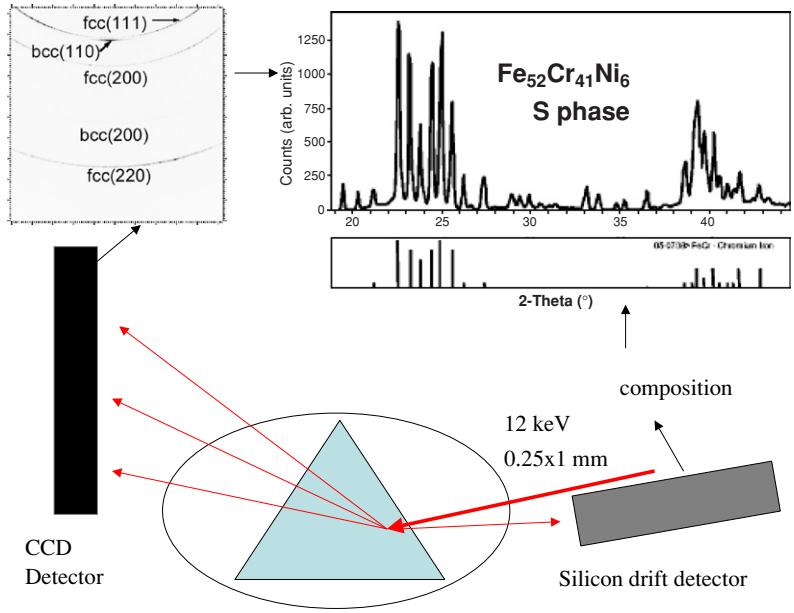

Figure 4. Schematic of XRD scanning experiment and data processing.

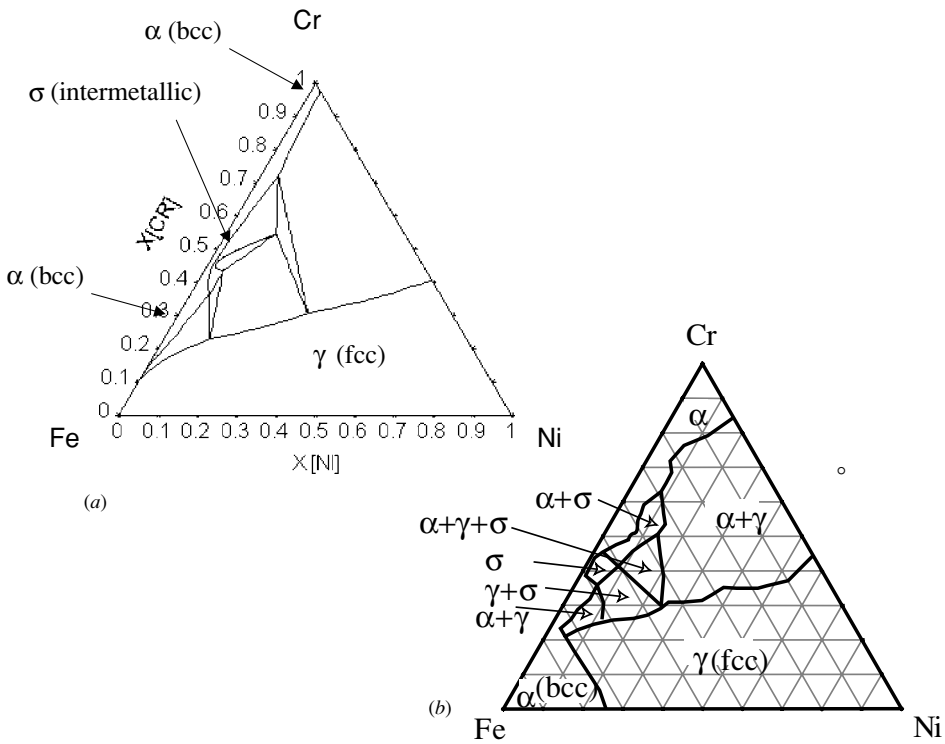

Figure 5. (*a*) Calculated ternary diagram of Ni–Fe–Cr system at 875 °C and (*b*) measured ternary diagram for sample interdiffused at 875 °C for 3 h and 20 min.

The experimentally measured phase distribution at an annealing temperature of 800 °C corresponds well to the equilibrium diagram calculated for the same temperature, indicating that equilibrium has been achieved. In addition, diffusion mobility is high at 600 °C as confirmed by the disappearance of the metastable phase and by the temperature dependence of the grain sizes, as shown in figure 7. The Scherer particle size equation [21] was used to calculate the grain size from the most intense peak of each phase with no corrections for instrumental resolution. Grain growth begins at 600 °C, which is also the temperature at which the 'α-Mn' phase disappears. At 400 °C and below, the samples are clearly not in equilibrium, since a significant portion of the observed composition spread is occupied by the metastable 'α-Mn' phase, thus providing options to study the phase properties. The great mobility at 600 °C opens the possibility of full

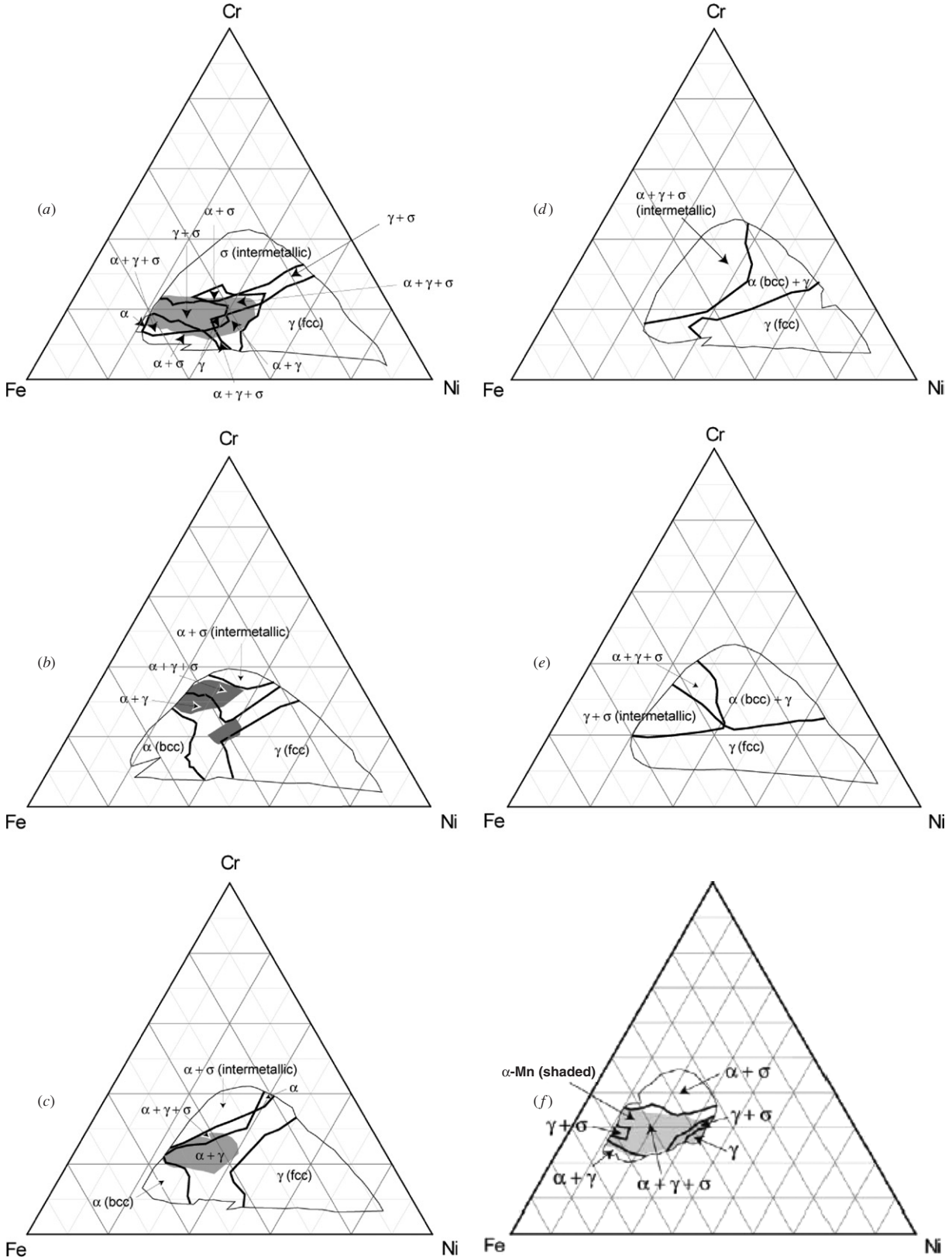

Figure 6. Ternary phase diagram for codeposited sample (*a*) as-deposited, and after 2 h annealing in vacuum at (*b*) 200 °C, (*c*) 400 °C, (*d*) 600 °C, (*e*) 800 °C. (*f*) Ternary phase diagram for as-deposited sample on a 50 mm substrate from [4].

alloying at a lower temperature than for the thick interdiffusion layer method, where annealing temperatures in the range of 825–875 °C were required [7].

The e-beam welding methods are still in development. The film thickness and e-beam parameters are far from optimal and may limit the obtained composition spread. For example,

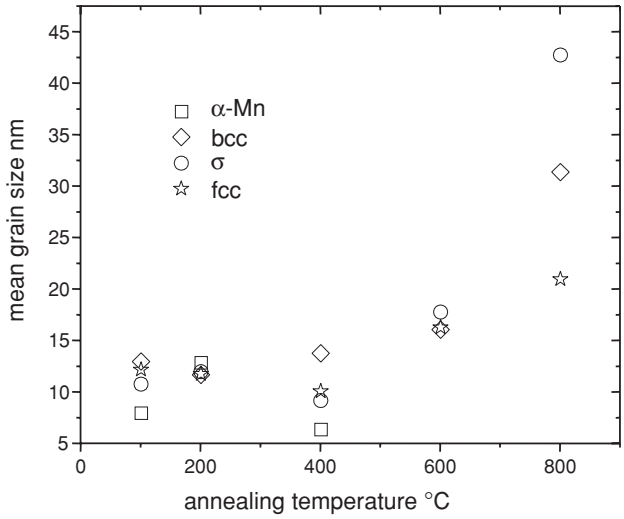

Figure 7. Diffraction particle size for observed phases versus annealing temperature as measured by x-ray technique.

one typical weld used for nanoindentation only had a Cr composition range of 5–25 at%. Increasing the e-beam current provided a deeper and larger weld and alloy region with smaller Cr concentration, but also produced significant surface roughness that made the nanoindentation measurements difficult. Preparation of samples with a higher Cr concentration by means of a thicker Cr layer may prove difficult because the Cr does not adhere well to the Ni substrate past a certain thickness. Instead, samples with higher Cr concentration were prepared by Ni films on Cr substrates. This EBW method may also be useful for ternary alloy preparation by using, for example, Cr- and Fe-deposited films wedged in different directions on the nickel substrate.

5. Testing of mechanical properties by nanoindentation

The libraries prepared by electron-beam welding were found to be best for nanoindentation measurements because the depth and width of the region to be tested were greater than typical sizes needed for nanoindentation experiments. The measured elastic modulus, E, and hardness, H, versus Cr concentration for five samples are shown in figure 8 by circles together with the data for bulk samples shown by triangles.

The results for the different libraries for the same composition are similar (within the experimental scatter), indicating that the properties of the alloy libraries depend only on the resulting alloy composition and are not sensitive to differences in the procedures used for library preparation, i.e., power setting of the welding e-beam, thickness of the deposited layer, which material (Ni or Cr) was used as substrate and which as deposited film. The scatter in the library data is related to sample roughness and the presence of multi-phase regions at some compositions. The last factor also contributes to scatter in the measurements of the bulk samples. The results for Cr concentration above 85 at% were found to be too scattered and will not be shown and discussed in this paper.

The measured moduli for bulk samples agree well with the results obtained for the library. The composition dependence

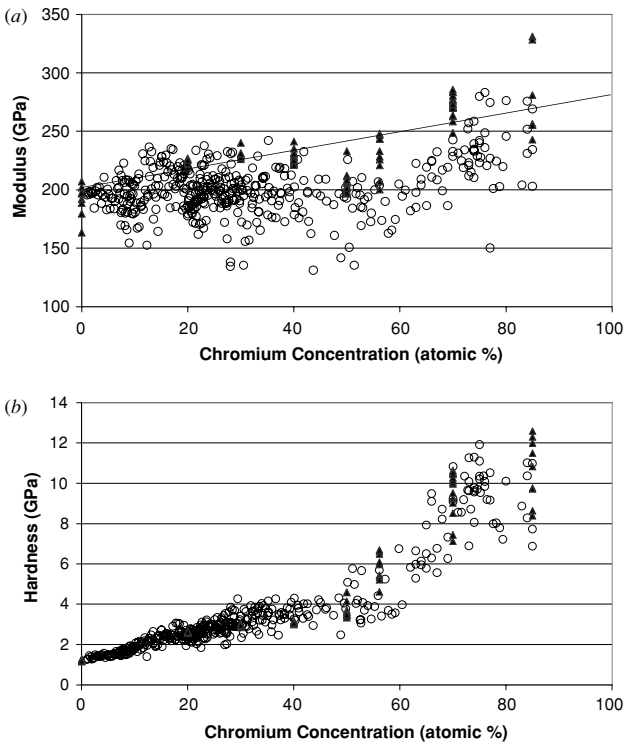

Figure 8. Nanoindentation measurements of (*a*) modulus and (*b*) hardness of EBW samples (open circles) and bulk standard (triangles) versus Cr composition. The line shows the expected modulus from the rule of mixtures.

of modulus is not trivial. The solid line through the data indicates the modulus expected from a simple 'rule of mixing' by using moduli for Ni and Cr, of 200 and 270 GPa, respectively [22]. For Cr concentrations below 30 at% the measured modulus follows the tendency expected from the mixing law, but is slightly lower than predicted. This may indicate problems with the accuracy of nanoindentation measurements, and some sample problems due to surface voids or contamination. The measured moduli are almost constant for Cr compositions from 30 to 60 at% but increase rapidly thereafter.

The hardness measurements also show good correlation between the EBW library and bulk samples. The hardness increase with Cr concentration correlates well with the modulus increase, i.e., hardness increases for Cr compositions below 30 at%, remains roughly constant from 30 to 50 at%, and then increases by a factor of 3 when the Cr concentration increases from 50 to 75 at%. The nanoindentation measurements have been confirmed by microhardness measurements which have been carried out on the same bulk samples. These measurements reproduce well the nanoindentation results.

The complicated dependences of modulus and hardness of the alloy on the composition are probably due to formation of a binary phase at chromium concentration between 40 and 85 at%. This preliminary assumption is based upon the formation of binary phase around a chromium concentration of about 40 at% according to the phase diagram as shown in figure 5(*a*). A careful characterization of the alloy microstructure will be performed in the future to understand the hardness and modulus dependence on Cr concentration.

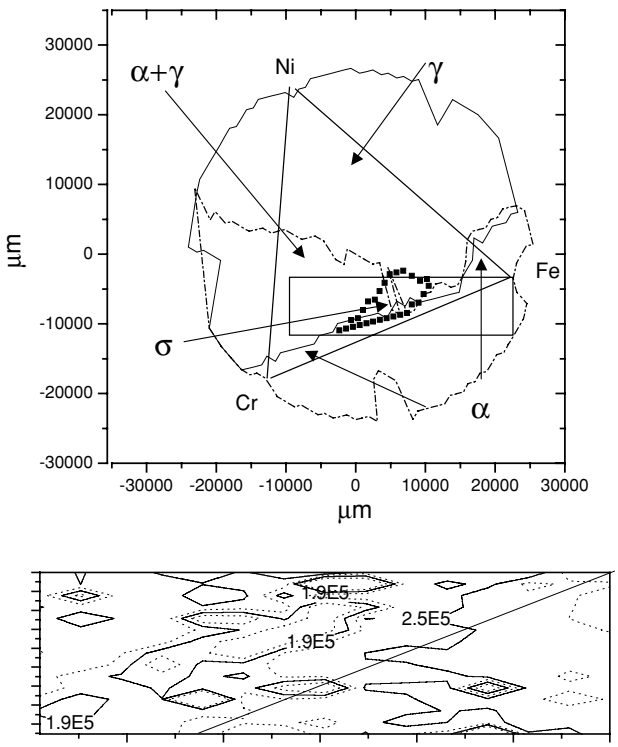

Figure 9. Boundary map for a ternary alloy library made by thick-layer interdiffusion. The location of the α phase is shown by the dashed line, γ by the solid line and σ by closed squares. The triangle indicates the location of the ternary library; the rectangle indicates the area where the nanoindentation mapping was performed. The contact stiffness map in N m^{-1} for this area for load 2.7 mN is shown in a separate panel as a contour map. The border of the ternary diagram for the map is shown by the diagonal line.

In general, nanoindentation measurements of the thin films on substrate have two problems: data scatter due to surface roughness [23] and influence of substrate on the measured modulus and hardness [24, 25]. These factors were significant in measurements of the alloy libraries made by interdiffusion and codeposition.

Nanoindentation measurements proved most difficult for the libraries prepared by interdiffusion. This complication was due to the relatively thin layer of Fe–Cr–Ni alloy produced, and also due to the surface becoming rough during annealing as a result of grain growth. Surface roughness produces scatter in nanoindentation measurements [23]. For these samples, the mechanical properties were screened to determine relative variations within the sample. Some of the screening results have been discussed in [18]. In figure 9, the results of 2D mapping of 15 × 15 contact stiffness measurements at a fixed load of 2.7 mN is shown for the region around the σ phase. The contact stiffness at fixed load is not very sensitive to surface roughness. The measured contact stiffness decreases in the σ phase from about 2.5×10^5 to 1.6×10^5 N m^{-1} relative to the nearby α phase. Assuming from the 'rule of mixing' that the changes in modulus are negligibly small, this corresponds to an increase in hardness of about 2.5 times, which is similar to earlier results [18] and agrees with the tendency observed in bulk samples [26].

The codeposited samples were only about 2 μm thick, but the flat surface made standard nanoindentation measurements much easier. The preliminary experiments performed for the libraries prepared by codeposition show little scatter, indicating no problems due to roughness and significant contact depth region where the influence of substrate is not important or can be taken into account [24]. This made the future investigations of the mechanical properties of the α-Mn phase possible.

6. Conclusion: benefits and limitations of the methods

The examples of combinatorial alloy development presented here show that there is some tradeoff between easy structural/chemical characterization over a wide area of the phase diagram and easy mechanical measurements. Mechanical measurements were easier to obtain for the codeposited samples than for annealed multilayer deposited samples, and they were easiest for the electron-beam-welded samples. Surface polishing may be additionally applied to EBW samples and should reduce roughness-related data scatter and possible effects of surface contamination.

Structural mapping of the full ternary diagram is easiest for samples made by interdiffusion, but more difficult for codeposited samples due to the limited range of composition that can be achieved. The additional benefit of codeposited libraries is the option of studying the non-equilibrium phases. The structural mapping of EBW samples is difficult because of limited composition spread in a single sample. Five samples were used to cover all possible binary compositions in these investigations, and the number of the samples will not be smaller than 2 with 2–3 welds on each sample even in perfect conditions. This amount will increase significantly for ternary library preparation by EBW.

Acknowledgments

Work sponsored by the US Department of Energy (US DOE), Division of Materials Sciences and Office of Industrial Technologies, Industrial Materials for the Future Program, under grant no DE-FC07-02ID14251. Oak Ridge National Laboratory (ORNL) is operated by UT-Battelle LLC, for the US DOE under contract no DE-AC05-00OR22725. The UNICAT facility at the Advanced Photon Source (APS) is supported by the University of Illinois at Urbana-Champaign, Materials Research Laboratory (US DOE, the State of Illinois-IBHE-HECA and the NSF), the Oak Ridge National Laboratory (US DOE under contract with UT-Battelle LLC), the National Institute of Standards and Technology (United States Department of Commerce) and UOP LLC. The APS is supported by the US DOE, Basic Energy Sciences, Office of Science under contract no W-31-109-ENG-38.

References

[1] Hanek J J 2004 *Appl. Surf. Sci.* **223** 1
[2] Adams E J, Xiang X D and Zhao J C 2002 *MRS Bull.* **27** 295
[3] Xiang X D 2004 *Appl. Surf. Sci.* **223** 54
[4] Collins P C, Banerjee R, Banerjee S and Fraser H L 2003 *Mater. Sci. Eng.* A **352** 118
[5] Cohen-Adad M Th, Gharbi M, Goutaudier C and Cohen-Adad R 1999 *J. Alloys Compounds* **289** 185
[6] Obermeier E 1997 *Mater. Res. Soc. Symp. Proc.* 39

[7] Rar A, Specht E D, George E P, Santella M L and Pharr G M 2004 *J. Vac. Sci. Technol.* A **22** 1788
[8] Christen H M, Silliman S D and Harshavardhan K S 2002 *Appl. Surf. Sci.* **189** 216
[9] Lula R A and Parr J G 1986 *Stainless Steel* (Metals Park, OH: American Society for Metals)
[10] Yamamoto Y, Takahashi R, Matsumoto Y, Chikyow T and Koinuma H 2004 *Appl. Surf. Sci.* **223** 9
[11] Specht E D, Rack P D, Rar A, Pharr G M, George E P and Hong H 2004 *Mater. Res. Soc. Symp. Proc.* **804** 45
[12] Oliver W C and Pharr G M 1992 *J. Mater. Res.* **7** 1564
[13] Rabe U, Amelio S, Kopycinska M, Hirsekorn S, Kempf M, Goken M and Arnold W 2002 *Surf. Interface Anal.* **33** 65
[14] Hurley D C, Tewary V K and Richards A J 2001 *Meas. Sci. Technol.* **12** 1486
[15] Specht E D, Rar A, Pharr G M, George E P, Zschack P, Hong H and Ilavsky J 2003 *J. Mater. Res.* **18** 2522
[16] Chen S L, Daniel S, Zhang F, Chang Y A, Yan X Y, Xie F Y, Schmid-Fetzer R and Oates W A 2002 *Calphad* **26** 175
[17] Hack K (ed) 1996 *The SGTE Casebook: Thermodynamics at Work* (London: The Institute of Materials) p 227
[18] Rar A, Specht E D, Meyer H M III, Santella M L, George E P and Pharr G M 2004 *Mater. Res. Soc. Symp. Proc.* **804** 63
[19] Simmonds M C, Newman R C, Fujimoto S and Colligon J S 1996 *Thin Solid Films* **279** 4
[20] Brandon J K, Brizard R Y, Chieh P C, McMillan R K and Pearson W B 1974 *Acta Crystallogr.* B **30** 1412
[21] Warren B E (ed) 1990 *X-Ray Diffraction* (New York: Dover) p 253
[22] Simmons G and Wang H 1971 *Single Crystal Elastic Constants and Calculated Aggregate Properties* (Cambridge, MA: MIT Press)
[23] Mencik J and Swain M V 1995 *J. Mater. Res.* **10** 1491
[24] Rar A, Song H and Pharr G M 2002 *Mater. Res. Soc. Symp. Proc.* **695** 431
[25] Nix W D 1997 *Mater. Sci. Eng.* A **234–236** 37
[26] Bain E C and Griffiths W E 1927 *Trans. AIME* **75** 166